CircHIPK3 promotes neuroinflammation through regulation of the miR-124-3p/STAT3/NLRP3 signaling pathway in Parkinson's disease

Yu-Juan Zhang[1,2,A,C,D,F], Wen-Kai Zhu[3,B,C], Fa-Ying Qi[3,B−D], Feng-Yuan Che[1,3,A,C,F]

[1] Institute of Clinical Medicine College, Guangzhou University of Chinese Medicine, China

[2] Department of Acupuncture, Linyi People's Hospital, China

[3] Department of Neurology, Linyi People's Hospital, China

A – research concept and design; B – collection and/or assembly of data; C – data analysis and interpretation;
D – writing the article; E – critical revision of the article; F – final approval of the article

Address for correspondence
Feng-Yuan Che
E-mail: chefy2020@163.com

Abstract

Background. Parkinson's disease (PD) is characterized as a neurodegenerative disease; however, the mechanisms regarding its pathogenesis have not been fully explored.

Objectives. To explore the role of circular RNA homeodomain interacting protein kinase 3 (circHIPK3) in the progression of PD.

Materials and methods. The circHIPK3 and microRNA-124 (miR-124) expression in human serum and cerebral fluid was detected using real-time quantitative reverse transcription polymerase chain reaction (qRT-PCR) in 92 PD patients and 95 controls. The circHIPK3 was overexpressed and/or silenced in cells to explore its molecular mechanisms and effects on neuroinflammation. The production of intracellular reactive oxygen species (ROS) was assessed using 2′,7′-dichlorodihydrofluorescein diacetate (DCFH-DA) staining. Interleukin 6 (IL-6), IL-1β and tumor necrosis factor alpha (TNF-α) production in BV2 cells after the indicated treatment was measured using enzyme-linked immunosorbent assay (ELISA). The protein expression of microglia markers (cluster of differentiation molecule 11b (CD11b) and ionized calcium-binding adapter molecule 1 (Iba-1)), pyroptosis-related factors, NLR family pyrin domain containing 3 (NLRP3), apoptosis-associated speck-like protein containing C-terminal caspase recruitment domain (ASC), and caspase-1, signal transducer and activator of transcription 3 (STAT3), and phosphorylated STAT3 (p-STAT3) were examined using western blot analysis. Furthermore, the interaction between circHIPK3, miR-124 and STAT3 was predicted with bioinformatics and examined using fluorescence in situ hybridization (FISH), luciferase reporter assays, RNA pull-down, and RNA immunoprecipitation (RIP).

Results. The expression of circHIPK3 in human serum and cerebral fluids was significantly higher than in controls, whereas miR-124 expression was drastically reduced. In addition, lipopolysaccharide (LPS)-treated BV2 cells exhibited higher expression of circHIPK3 and lower miR-124 expression. The SH-SY5Y cells exhibited a significantly impaired viability and elevated apoptotic rate, along with an upregulation of circHIPK3 and a downregulation of miR-124 expression after being treated with supernatants collected from LPS-treated BV2 cells. The upregulation of circHIPK3 increased IL-6, IL-1β and TNF-α secretion in BV2 cells. The protein expressions of microglia markers (CD11b and Iba-1), as well as pyroptosis-related factors, NLRP3, caspase-1, and ASC, were also increased following the expression of circHIPK3. All these effects were reversed by the addition of miR-124.

Conclusions. The circHIPK3 enhances neuroinflammation by sponging miR-124 and regulating the miR-124-mediated STAT3/NALP3 pathway in PD.

Key words: Parkinson's disease, NLRP3, miR-124, neuroinflammation, circHIPK3

Background

Parkinson's disease (PD) is characterized as a progressive and chronic neurodegenerative disease that affects middle-aged and elderly people.[1] Based on reports, the incidence of PD is 1% in people over 65 years of age and 5% in those older than 85.[1] The loss of dopaminergic neurons in the substantia nigra pars compacta (SNpc) leads to the development of the clinical features of PD.[2] These include motor symptoms, such as bradykinesia, akinesia, resting tremor, postural instability, and rigidity. In addition, non-motor features include fatigue, pain, olfactory dysfunction, autonomic dysfunction, sleep disorders, psychiatric symptoms, and cognitive impairment.[3] Although many studies have been performed, the pathogenesis of PD is not completely understood, and no drugs are available to alleviate the progression of the disease.

In recent years, neuroinflammation has been identified as a major factor associated with the pathogenesis of PD.[4] Compared to healthy controls, the samples of cerebrospinal fluid (CSF) and substantia nigra (SN) collected from PD patients exhibited relatively high levels of cytokines and complement.[5] Inflammasomes, specifically the NLR family pyrin domain containing 3 (NLRP3) inflammasome generated by caspase-1, apoptosis-associated speck-like protein containing C-terminal caspase recruitment domain (ASC) adaptor protein and NLRP3 are significantly involved in the pathogenesis and progression of PD.[6] As one of the innate immune cells which reside in the central nervous system (CNS), microglia are involved in both normal and pathologic conditions of the CNS. Additionally, the protective and toxic effects of neuroinflammation caused by the activation of microglia in the brain have been observed.[7,8] Studies have also identified that the NLRP3 inflammasome functions in microglia but not in astrocytes.[9] Therefore, the inhibition of microglia inflammation by targeting NLRP3 may be a potential treatment option in PD.

As a non-coding RNA, circular RNAs (circRNAs) are generated by back-splicing from precursor messenger RNA (mRNA) and expressed in specific tissues in mammals.[10,11] Accumulating evidence indicates that circRNAs exert specific biological functions and participate in various pathophysiologic and physiologic processes in neoplastic cells.[12] It has also been proven that because of the existence of binding sites with microRNA (miRNA), circRNAs exert a regulatory role in diseases by controlling the expression of miRNA associated with diseases through a direct interaction.[12]

Growing evidence has implicated circRNAs to significantly participate in the pathogenesis of Alzheimer's disease,[13] stroke,[14] PD,[15] etc. Recently, circRNAs were considered potential targets for PD treatment because of their changing expression during the development of PD.[16] For example, an elevated expression of circSLC8A1 was observed in PD patients and cells after oxidative stress.[17] In another study, the significant upregulation and close connection of circzip-2 with the pathogenesis of PD was found.[18] Moreover,

Ghosal et al. indicated that ciRS-7 was significantly involved in the nucleoprotein enrichment pattern of miR-7 in PD.[19]

The circRNA homeodomain interacting protein kinase 3 (circHIPK3, circRNA ID: hsa_circ_0000284) has been implicated to facilitate inflammation in various disease states.[20] Through a direct interaction with miR-561 and miR-192, circHIPK3 powerfully enhances the activation of the toll-like receptor 4 (TLR4) pathway and macrophage NLRP3 inflammasomes in gouty arthritis.[21] At the same time, a significant increase in the expression of circHIPK3 in lipopolysaccharide (LPS)-treated H9c2 cells and LPS-induced myocarditis in animals was observed in vitro and in vivo, and the LPS-induced myocarditis was improved by silencing circHIPK3.[22] An increased expression of circHIPK3 was positively correlated with the degree of neuropathic pain in type II diabetic patients.[23] In diabetic rats, the downregulation of circHIPK3 effectively attenuated neuropathic pain, suggesting the involvement of circHIPK3 in neuroinflammation.[23] However, whether circHIPK3 promotes neuroinflammation following microglia activation in PD remains unknown.

The miR-124 has been the focus of studies on the progression of PD. The microRNA-124 (miR-124) expression was identified in human brain tissues, and the involvement of miR-124 in neurotransmission, synapse morphology and neurogenesis has been found.[24] Previous studies have also shown that miR-124 regulates oxidative damage, mitochondrial dysfunction, neuroinflammation, autophagy, and cell survival in PD.[25] Decreased concentrations of miR-124 in plasma may be considered a diagnostic marker for PD.[26] These findings suggested that miR-124 performs a neuroprotective role in PD and has a therapeutic value.[27]

The signal transducer and activator of transcription 3 (STAT3) is associated with controlling inflammation and immunity, including those in microglia.[28] The activation of STAT3 enhances the expression of inflammation-associated genes and can induce a reduction in dopaminergic neurons, subsequently leading to PD symptoms in mice.[29,30] In addition, through direct interaction with the promotor of NLRP3, STAT3 can enhance the expression of NLRP3 and promote neuronal pyroptosis, leading to neuronal damage.[31]

Objectives

This study aims to explore the potential molecular mechanisms regulating circHIPK3, miR-124 and NLRP3 in inflammation observed in PD patients.

Materials and methods

Patients

The expression of circHIPK3 and miR-124 in blood samples obtained from 92 PD patients was determined. Patients with other neurodegenerative diseases such as Alzheimer's

disease, Huntington's disease and amyotrophic lateral sclerosis were excluded from the study. Additionally, patients with unstable comorbidities, a history of receiving deep brain stimulation and younger than 18 years were also excluded. A lumbar puncture, blood sample collection, standardized detailed neurologic examination, and other ancillary investigations, such as magnetic resonance imaging (MRI), as well as structured interviews, were performed for all patients before the beginning of the study. The protocols for this study were reviewed and approved before the initiation of the study by the Linyi People's Hospital ethics committee (No. of approval 20210045). Patients (n = 95, age > 40) without any neurological and inflammatory disorders were enrolled as a control group. Patients from the control group underwent a lumbar puncture to exclude any potential or suspected neurological disorders. Written informed consent was signed by the patients enrolled in this study. This study complied with the Declaration of Helsinki.

Sample preparation and real-time quantitative reverse transcription polymerase chain reaction

Lumbar puncture was performed using the standard technique. Collected CSF without blood contamination was immediately frozen at –80°C and kept for further usage. The numbers of leukocytes and erythrocytes in the collected CSF samples were no more than 5 cells/µL and 200 cells/µL, respectively. After overnight fasting and incubation for 2–3 h at room temperature (RT), the venous blood was centrifuged at 1900 g for 20 min. Then, the serum was stored for further analysis at –80°C. The total RNA in the serum samples was extracted using the TaKaRa RNA Extraction Kit (TaKaRa, Tokyo, Japan).

The purity and concentrations of RNA were evaluated using the Nanodrop-1000 (Thermo Fisher Scientific, Waltham, USA). A PrimeScript™ RT reagent Kit (TaKaRa) was employed to perform a reverse transcription of the extracted mRNA to complementary DNA (cDNA). The SYBR® Premix Ex Taq™ II (TaKaRa) was used to perform the real-time quantitative reverse transcription polymerase chain reaction (qRT-PCR). The primers were designed using Primer Premier v. 6.0 software (PREMIER Biosoft, San Francisco, USA) and the sequences of these primers were listed as follows: circHIPK3 forward: 5'-TATGTTGGTGGATCCTGTTCGGCA-3', reverse: 5'-TGGTGGGTAGACCAAGACTTGTGA-3'; glyceraldehyde-3-phosphate dehydrogenase (GAPDH) forward: 5'-ACCACAGTCCATGCCATCAC-3', reverse: 5'-TCCACCACCCTGTTGCTGTA-3'; miR-124 forward: 5'-TCTTTAAGGCACGCGGTG-3', reverse: 5'-TATGGTTTTGACGACTGTGTGAT-3'; and U6 forward: 5'-CTCGCTTCGGCAGCACA-3', reverse: 5'-AACGCTTCACGAATTTGCGT-3'. The circHIPK3 and miR-124 expressions were calculated using the $2^{-\Delta\Delta Ct}$ method. The GAPDH and U6 expressions were used to normalize the circHIPK3 and miR-124 expressions, respectively.

Cells and cell culture

The SH-SY5Y and BV2 cells were cultured in Roswell Park Memorial Institute (RPMI) 1640 medium (Gibco, Waltham, USA) containing glucose (5 mM), fetal bovine serum (FBS, 10%; Gibco) and streptomycin/penicillin (1%; Gibco). The medium was replaced every 2 days and the cells that reached 80% confluence were collected for further experiments.

Conditioned medium-induced neurotoxicity

After 48 h of incubation with LPS (1 µg/mL), the supernatants of the BV2 were collected. To remove the cellular debris, 5-min centrifugation at 2500 rpm was conducted. The collected supernatants were then stored at –80°C and used as the conditioned medium (CM) in further experiments. For CM-induced neurotoxicity, the SH-SY5Y cells were incubated with CM for another 24 h after a 24-hour culture in a normal medium. The neuronal viability was then assessed.

Measurement of cell viability

The cells were cultured overnight before the measurement. After a 4-hour incubation with 500 µg/mL of MTT solution at 37°C in the dark, the medium was replaced with dimethyl sulfoxide (DMSO). After a 10-minute shaking, the absorbance was read using a microplate reader (BioTek, Winooski, USA) at 450 nm.

Determination of cell apoptosis

Annexin V staining was conducted to evaluate the apoptosis rate of SH-SY5Y cells. Briefly, after washing and centrifugation, the cells were suspended in a 1× Annexin V binding buffer PI (5 µL; BioVision, Waltham, USA) and Annexin V (5 µL) was added and stained at RT for 15 min. The apoptosis rate was detected using flow cytometry.

Cell transfection

A miR-124 mimic was obtained from Guangzhou Riobo-Bio Co., Ltd. (Guangzhou, China). A siRNA (5'-CUACAGGUAUGGCCUCACA-3') specifically targeted to circHIPK3 was transfected into the BV2 cells to silence the expression of circHIPK3. The cell transfection was conducted using Lipofectamine™ 3000 (Thermo Fisher Scientific).

Detection of reactive oxygen species

Reactive oxygen species (ROS) in the cells were evaluated by 2',7'-dichlorodihydrofluorescein diacetate (DCFH-DA) staining. Briefly, after a 30-minute culture with 10 µM of DCFH-DA at 37°C, the level of ROS in the BV2 cells with different treatments was measured at excitation/emission = 485/535 nm.

Western blot analysis

After a 20-minute centrifugation at 12,000 g, the protein concentrations of the supernatant were determined. The samples (30 μg per sample) were loaded into a 10–12% sodium dodecyl–sulfate polyacrylamide gel electrophoresis (SDS–PAGE). Next, after transferring onto a polyvinylidene difluoride (PVDF) membrane, the protein bands were blocked in 5% fat-free milk for 1 h at RT. Then, after overnight incubation with the indicated primary antibodies at 4°C, washing 3 times with phosphate-buffered saline with Tween® detergent (PBST), and a 1-hour incubation with horseradish peroxidase (HRP)-conjugated secondary antibodies at RT, the protein bands and signals were detected using an enhanced chemiluminescence detection system (Pierce, Rockford, USA). The antibodies used were as follows: GAPDH (1:1000; Abcam, Cambridge, UK), phosphorylated STAT3 (p-STAT3, 1:1000; Abcam), STAT3 (1:1000; Abcam), ASC (1:1000; Cell Signaling Technology, Danvers, USA), caspase-1 (1:800; Cell Signaling Technology), NLRP3 (1:1000; Cell Signaling Technology), ionized calcium-binding adapter molecule 1 (Iba-1, 1:800; Abcam), and cluster of differentiation molecule 11b (CD11b, 1:1000; Abcam). All protein expressions were normalized to GAPDH.

Enzyme-linked immunosorbent assay

The enzyme-linked immunosorbent assay (ELISA) kits for tumor necrosis factor alpha (TNF-α), interleukin-1β (IL-1β) and IL-6 (R&D Systems, Minneapolis, USA) were purchased to examine their production from BV2 cells in the supernatant.

Luciferase assay

The cDNA of circHIPK3 containing predicted binding or mutation sites was obtained using PCR amplification. The purified PCR fragment was then inserted into a pGL3 vector (Promega, Madison, USA) at XhoI/KpnI sites in order to generate the target luciferase reporter plasmid. We named these vectors circHIPK3-WT and circHIPK3-MUT, respectively. Similarly, the magnification of miR-124 3'-UTR of the wild-type STAT3 was performed using PCR, and then it was loaded on a pGL3 vector immediately downstream to the firefly luciferase reporter gene. The complex was called pGL3-WT-STAT3-3'UTR. Next, we mutated the miR-124 binding site of STAT3 3'-UTR using the Site-Directed Mutagenesis Kit (Abcam, Cambridge, UK) and inserted it into another PGL3 at the same location. The mutant is known as PGL3-MUT-STAT3-3'UTR. Forty-eight well plates were used to inoculate BV2 cells. When the convergence reached 50%, 500 ng of luciferin reporter vector was co-transfected with 30 nM of miR-124 mimic or negative control (NC)-mimic using Lipofectamine™ 2000 (Thermo Fisher Scientific). After 48 h of culture, the relative luciferase activities were determined.

Fluorescence in situ hybridization

The circHIPK3 was labeled with Cy5, the DNA Oligo Probe (GenePharma, Suzhou, China) was labeled with 5-carboxyfluorescein (FAM), and the nucleus was back-stained with 4,6-diamidino-2-phenylindole dihydrochloride (DAPI; GenePharma), which was used for fluorescence in situ hybridization (FISH) detection. After staining, the results were observed and the images were captured under a Leica SP5 confocal microscope (Leica, Wetzlar, Germany).

RNA immunoprecipitation (RIP)

After overnight incubation with anti-immunoglobulin G (IgG) (Merck Millipore, Burlington, USA) or anti-STAT3 (Ago2) antibodies, the RNA-protein complex was precipitated with protein A agarose beads, followed by RNA extraction and qRT-PCR detection. The negative control was normal IgG.

RNA pull-down assay

We lysed human BV2 cells transfected with miR-124 mimics and incubated them with a circHIPK3 biotin-conjugated probe that was bound to magnetic beads for 2 h to pull down the miR-124. Then, the pulled-down RNA was purified. The miR-124 biotin-conjugated probe was treated as before.

Northern blot

The RNA samples were separated using a polyacrylamide gel and transferred to Amersham™ Hybond™-N+ nylon membrane (Amersham Biosciences, Amersham, UK). After fixation with purple coupling, PerfectHyb™ (Sigma-Aldrich, St. Louis, USA) was pre-hybridized and incubated with P32 probes generated using the StarFire® Nucleic Acid Labeling System (Integrated DNA Technologies, Coralville, USA). The U6 or β-actin were used as the control.

Statistical analyses

All the obtained data were processed and analyzed using GraphPad Prism v. 7.0 (GraphPad Software, San Diego, USA). Shapiro–Wilk test was used to test the normal distribution, whereas F-test was applied to check the homogeneity variance among the groups (Supplementary File). The χ^2 test was used to investigate the distribution of sexes. Mann–Whitney U test was conducted for the comparisons between the 2 groups in terms of gene expression collected in clinical samples. When 3 or more groups were compared, Kruskal–Wallis test was used, followed by Dunn's test for post hoc analysis. For cell experiments, given that the sample size was very small and that checking the normal distribution has little power, nonparametric tests were used (Mann–Whitney U test or Kruskal–Wallis test followed

by Dunn's test). The values were expressed as median (interquartile range (IQR)) or data point plots (central tendency measure and interval). Spearman's analysis was used to test the correlation between the expression of 2 genes. A value of $p < 0.05$ was considered statistically significant.

Results

CircHIPK3 expression was elevated in PD patients, LPS-induced BV2 cells and conditioned SH-SY5Y medium

The demographic data of PD patients and controls are listed in Table 1. There were no significant differences with regard to age, sex distribution and body mass index (BMI) between PD patients and controls (Table 1).

The expression of circHIPK3 and miR-124 in human blood and CSF was detected with qRT-PCR. The qRT-PCR analysis showed that the expression of circHIPK3 in blood and CSF samples was significantly increased in PD patients compared to controls (blood: Mann–Whitney U test, U = 0, $p < 0.001$; CSF: Mann–Whitney U test, U = 0, $p < 0.001$; Fig. 1A,C). On the other hand, the expression of miR-124 in the blood and CSF samples was markedly decreased in PD patients compared to controls (blood: Mann–Whitney U test, U = 0, $p < 0.001$; CSF: Mann–Whitney U test, U = 0, $p < 0.001$; Fig. 1B,D; Table 2 – No. 1–4). Both circHIPK3 expression in blood and CSF samples were negatively correlated with miR-124 expression (blood: Spearman's correlation, r = −0.402, $p < 0.001$; CSF: Spearman's correlation, r = −0.447, $p < 0.001$; Fig. 1E,F; Table 2 – No. 5,6).

On the other hand, the expression of circHIPK3 was significantly higher in cells after LPS treatment compared to cells without the addition of LPS (Mann–Whitney U test, U = 0, $p = 0.002$), where miR-124 expression was drastically decreased (Mann–Whitney U test, U = 0, $p = 0.004$; Fig. 2A,B). In addition, a significantly reduced cell viability (Mann–Whitney U test, U = 0, $p = 0.002$) and increased cell apoptosis (Mann–Whitney U test, U = 0, $p = 0.007$) were observed in SH-SY5Y cells after CM treatment in comparison to non-treated control cells (Fig. 2C–F). In addition, circHIPK3 was upregulated (Fig. 2C; Mann–Whitney U test, U = 0, $p = 0.002$) and miR-124 expression was decreased (Mann–Whitney U test, U = 1, $p = 0.007$; Fig. 2D; Table 2 – No. 7–12).

CircHIPK3 enhanced ROS production

To clarify the regulatory roles of circHIPK3 on oxidative stress in cells, ROS content was evaluated. In comparison to control cells, the cells treated with LPS exhibited significantly higher levels of ROS (Kruskal–Wallis test, H(4) = 27.87, $p < 0.001$; Dunn's post hoc test, $p < 0.001$; Fig. 3A,B,F). The overexpression of circHIPK3 in transfection cells promoted significantly higher ROS levels (Dunn's post hoc test, $p < 0.001$), while adding miR-124 mimic stopped the LPS-stimulated production of ROS (Fig. 3C,E,F). In contrast, the silencing of circHIPK3 drastically decreased the LPS-stimulated production of ROS (Dunn's post hoc test, $p = 0.008$; Fig. 3D,F). These findings indicate that increases ROS levels in BV2 cells (Table 2 – No. 13).

CircHIPK3 promoted microglial activation and pyroptosis through the activation of STAT3 signaling

The association of circHIPK3 with inflammation and the activation of microglia was explored through the overexpression or knocking down of circHIPK3 in BV2 cells following LPS stimulation for 12 h. In comparison to the control cells, LPS-stimulated cells exhibited significantly increased CD11b, Iba-1, pyroptosis-related factors, NLRP3, caspase-1, and ASC expression (CD11b: Kruskal–Wallis test, H(4) = 25.16, $p < 0.001$; Iba-1: Kruskal–Wallis test, H(4) = 24.13, $p < 0.001$; NLRP3: Kruskal–Wallis test, H(4) = 22.58, $p < 0.001$; caspase-1: Kruskal–Wallis test, H(4) = 24.13, $p < 0.001$; ASC: Kruskal–Wallis test, H(4) = 28.47, $p < 0.001$). The results of Dunn's post hoc test were $p = 0.024$, $p = 0.036$, $p = 0.017$, $p = 0.02$, and $p = 0.027$, respectively. The upregulation of circHIPK3 further increased CD11b and Iba-1 expression as well as NLRP3, caspase-1 and ASC (Dunn's post hoc test: $p = 0.018$, $p = 0.009$, $p = 0.019$, $p = 0.034$, $p = 0.016$, respectively). The addition of miR-124 mimic reversed these effects. On the other hand, the LPS-induced expression of CD11b, Iba-1 and pyroptosis-related factors was dramatically reduced by the downregulation of circHIPK3 in LPS-treated cells (Dunn's post hoc test: $p = 0.034$, $p = 0.024$, $p = 0.036$, $p = 0.018$, $p = 0.038$, respectively; Fig. 4A–C). Last, we found that LPS stimulation significantly upregulated the expression of total STAT3 and p-STAT3 in comparison to control cells (STAT3: Kruskal–Wallis test, H(4) = 20.15, $p < 0.001$; p-STAT3: Kruskal–Wallis test, H(4) = 22.46, $p < 0.001$;

Table 1. Basic comparison between Parkinson's disease (PD) patients and controls

Demographic items	PD (n = 92)	Controls (n = 95)	U/χ²	p-value
Age	66.2 (60.1–71.5)	65.0 (60.0–69.2)	U = 3659	0.066
Sex (female/male)	38/54	40/55	0.012 (df = 1)	0.911
BMI [kg/cm²]	21.7 (19.6–23.4)	22.5 (19.9–25.5)	U = 3894	0.103
Disease duration since first symptoms [months]	22.0 (15.9–29.5)	–	–	–

df – degrees of freedom; BMI – body mass index. Age, BMI and disease duration were expressed as median (interquartile range (IQR)).

320

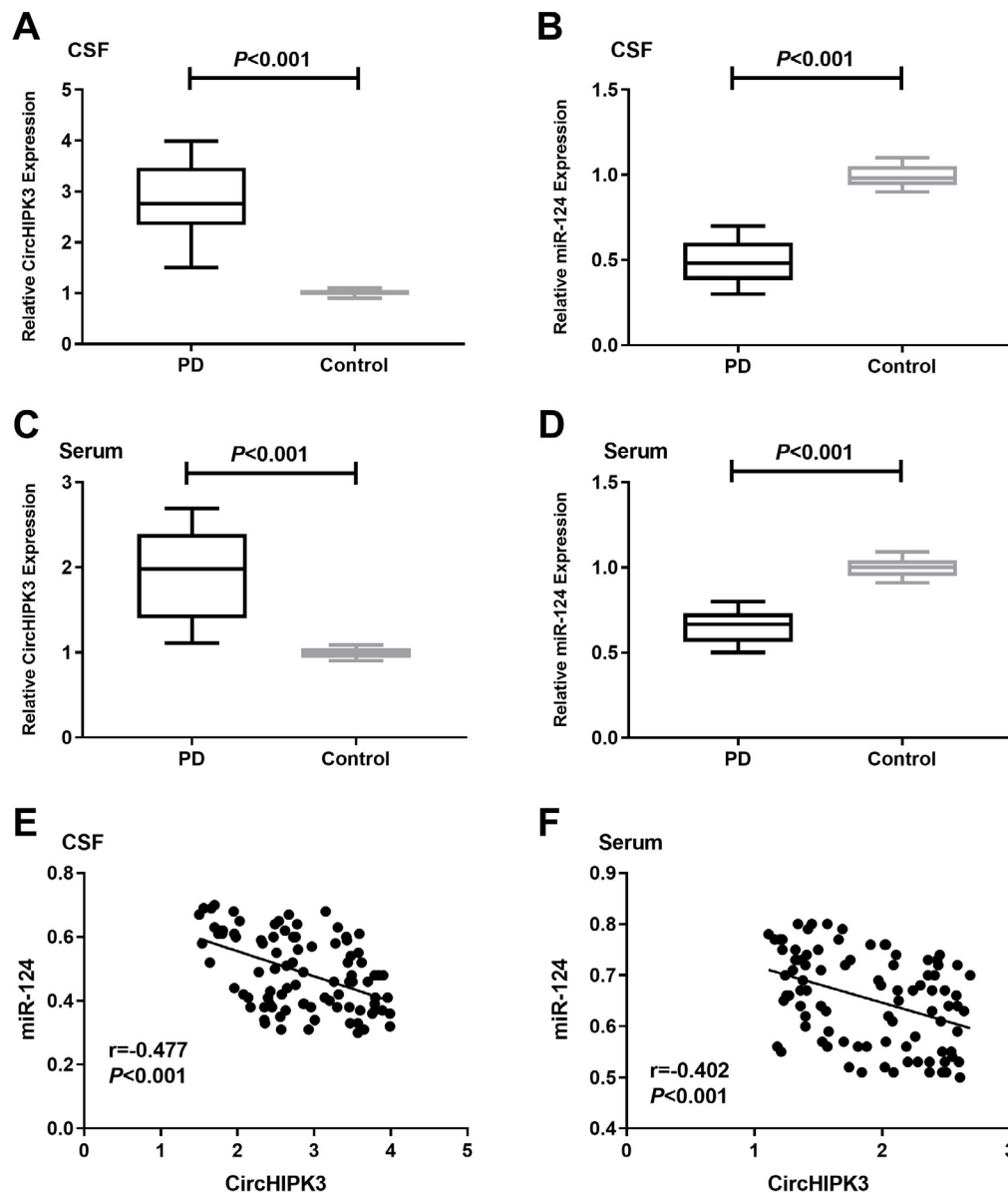Y. Zhang et al. CircHIPK3 in Parkinson's disease

Fig. 1. A. Relative cerebrospinal fluid (CSF) circular RNA homeodomain interacting protein kinase 3 (circHIPK3) expression between Parkinson's disease (PD) patients and control group; B. Relative microRNA-124 (miR-124) expression between PD and control group; C. Relative serum circHIPK3 expression between PD and control group. Results were statistically analyzed using Mann–Whitney U test. Data were expressed as median, Q3 (75% percentile), Q1 (25% percentile), interquartile range (Q3–Q1), and minimum and maximum values; D. Relative serum miR-124 expression between PD and control group; E. Correlation of miR-124 and circHIPK3 expression in CSF; F. Correlation of miR-124 and circHIPK3 expression in serum. Results were statistically analyzed using Spearman's correlation

Dunn's post hoc test: p = 0.005 and p = 0.008, respectively; Table 2 – No. 14–18). The overexpression of circHIPK3 further enhanced LPS-stimulated total STAT3 and p-STAT3 expression (Dunn's post hoc test: p = 0.036, p = 0.021, respectively), while adding miR-124 mimic could reverse these effects. Silencing of circHIPK3 decreased the expression of total STAT3 and p-STAT3 expression compared to the LPS group (Dunn's post hoc test: p = 0.027, p = 0.015, respectively; Fig. 4A,D; Table 2 – No. 19,20). Based on our results, we concluded that circHIPK3 exerted its promotive effect on the activation and pyroptosis of LPS-treated BV2 cells through the regulation of STAT3 signaling.

CircHIPK3 promoted inflammatory cytokine levels in BV2 cells

As shown in Fig. 4, in comparison to the control cells, the cells after LPS treatment exhibited a significantly enhanced expression of IL-6, IL-1β and TNF-α (IL-6: Kruskal–Wallis test, H(4) = 23.15, p < 0.001; IL-1β: Kruskal–Wallis test, H(4) = 29.18, p < 0.001; TNF-α: Kruskal–Wallis test, H(4) = 30.23, p < 0.001; Dunn's post hoc test: p = 0.005, p = 0.008, p = 0.004, respectively). Additionally, the secretion of IL-6, IL-1β and TNF-α stimulated by LPS was significantly enhanced and impaired by the overexpression of circHIPK3 and miR-124 mimic transfection, respectively (Dunn's post hoc test: p < 0.001, p = 0.006, p < 0.001, respectively). On the other hand, silencing circHIPK3 significantly decreased the production of IL-6, IL-1β and TNF-α stimulated by LPS (Dunn's post hoc test: p = 0.023, p = 0.016, p = 0.041, respectively; Fig. 5A–C; Table 2 – No. 21–23).

STAT3 was the target gene of miR-124

To predict the potential targets and binding sites of miR-124, TargetScan (http://www.targetscan.org) was used.

Table 2. Statistical results

Comparison items	Statistical method	Statistical value	p-value
1. CircHIPK3 CSF (PD vs controls) (Fig. 1A)	Mann–Whitney U test	U = 0	<0.001
2. MiR-124 CSF (PD vs controls) (Fig. 1B)	Mann–Whitney U test	U = 0	<0.001
3. CircHIPK3 serum (PD vs controls) (Fig. 1C)	Mann–Whitney U test	U = 0	<0.001
4. MiR-124 serum (PD vs controls) (Fig. 1D)	Mann–Whitney U test	U = 0	<0.001
5. Correlation of circHIPK3 expression and miR-124 expressions in CSF (Fig. 1E)	Spearman's correlation	r = −0.447	<0.001
6. Correlation of circHIPK3 expression and miR-124 expressions in serum (Fig. 1F)	Spearman's correlation	r = −0.402	<0.001
7. CircHIPK3 expression between BV2 and LPS-induced BV2 (Fig. 2A)	Mann–Whitney U test	U = 0	0.002
8. MiR-124 expression between BV2 and LPS-induced BV2 (Fig. 2B)	Mann–Whitney U test	U = 0	0.004
9. CircHIPK3 expression between SH-SY5Y and SH-SY5Y+LPS BV2 (Fig. 2C)	Mann–Whitney U test	U = 0	0.002
10. MiR-124 expression between SH-SY5Y and SH-SY5Y+LPS BV2 (Fig. 2D)	Mann–Whitney U test	U = 1	0.007
11. MTT between SH-SY5Y and SH-SY5Y+LPS BV2 (Fig. 2E)	Mann–Whitney U test	U = 0	0.003
12. Apoptosis rate between SH-SY5Y and SH-SY5Y+LPS BV2 (Fig. 2H)	Mann–Whitney U test	U = 0	0.001
13. ROS production (Fig. 3F)	Kruskal–Wallis test	Kruskal–Wallis H statistic = 27.87	<0.001
14. CD11b protein expression (Fig. 4B)	Kruskal–Wallis test	Kruskal–Wallis H statistic = 25.16	<0.001
15. Iba-1 protein expression (Fig. 4B)	Kruskal–Wallis test	Kruskal–Wallis H statistic = 24.13	<0.001
16. NLPRP3 protein expression (Fig. 4C)	Kruskal–Wallis test	Kruskal–Wallis H statistic = 22.58	<0.001
17. Caspase-1 protein expression (Fig. 4C)	Kruskal–Wallis test	Kruskal–Wallis H statistic = 29.16	<0.001
18. ASC protein expression (Fig. 4C)	Kruskal–Wallis test	Kruskal–Wallis H statistic = 28.47	<0.001
19. STAT3 protein expression (Fig. 4D)	Kruskal–Wallis test	Kruskal–Wallis H statistic = 20.15	<0.001
20. p-STAT3 protein expression (Fig. 4D)	Kruskal–Wallis test	Kruskal–Wallis H statistic = 22.46	<0.001
21. TNF-α ELISA (Fig. 5A)	Kruskal–Wallis test	Kruskal–Wallis H statistic = 23.15	<0.001
22. IL-1β ELISA (Fig. 5B)	Kruskal–Wallis test	Kruskal–Wallis H statistic = 29.18	<0.001
23. IL-6 ELISA (Fig. 5C)	Kruskal–Wallis test	Kruskal–Wallis H statistic = 30.23	<0.001
24. STAT3 WT relative luciferase activity (Fig. 6B)	Kruskal–Wallis test	Kruskal–Wallis H statistic = 19.55	<0.001
25. STAT3 MUT relative luciferase activity (Fig. 6B)	Kruskal–Wallis test	Kruskal–Wallis H statistic = 0.43	0.933
26. STAT3 mRNA expression (Fig. 6D)	Kruskal–Wallis test	Kruskal–Wallis H statistic = 19.59	<0.001
27. CircHIPK3 WT relative luciferase activity (Fig. 7B)	Kruskal–Wallis test	Kruskal–Wallis H statistic = 19.51	<0.001
28. CircHIPK3 MUT relative luciferase activity (Fig. 7B)	Kruskal–Wallis test	Kruskal–Wallis H statistic = 0.41	0.935
29. MiR-124 relative expression (Fig. 7D)	Kruskal–Wallis test	Kruskal–Wallis H statistic = 22.68	<0.001
30. MiR-124 RIP (Fig. 8B)	Kruskal–Wallis test	Kruskal–Wallis H statistic = 11.67	<0.001
31. CircHIPK3 RIP (Fig. 8B)	Kruskal–Wallis test	Kruskal–Wallis H statistic = 11.63	<0.001
32. MiR-124 RNA pull-down (Fig. 8C)	Mann–Whitney U test	U = 0	0.002
33. CircHIPK3 RNA pull-down (Fig. 8D)	Mann–Whitney U test	U = 0	0.002

CSF – cerebrospinal fluid; PD – Parkinson's disease; circHIPK3 – circRNA homeodomain interacting protein kinase 3; miR-124 – microRNA-124; LPS – lipopolysaccharide; ROS – reactive oxygen species; CD11b – cluster of differentiation molecule 11b; Iba-1 – ionized calcium-binding adapter molecule 1; NLRP3 – NLR family pyrin domain containing 3; ASC – apoptosis-associated speck-like protein containing C-terminal caspase recruitment domain; STAT3 – signal transducer and activator of transcription 3; p-STAT3 – phosphorylated STAT3; TNF-α – tumor necrosis factor alpha; ELISA – enzyme-linked immunosorbent assay; IL – interleukin; MTT – 3-(4,5-dimethyl-2-thiazolyl)-2,5-diphenyl-2-H-tetrazolium bromide; RIP – RNA-binding protein immunoprecipitation; MUT – mutant-type; WT – wild-type.

As shown in Fig. 6A, the potential binding sites between miR-124 and the 3'-UTR regions of STAT3 were found. The sequences of MUT-STAT-3'-UTR are shown in Fig. 6A. Luciferase demonstrated that in comparison to the control cells (Kruskal–Wallis test, H(3) = 19.55, p < 0.001), miR-124 mimic transfection significantly reduced the activity of luciferase (Dunn's post hoc test: p = 0.033). Also,

the transfection of anta-miR-124 dramatically enhanced the luciferase activity in cells transfected with WT-STAT-3'-UTR (Dunn's post hoc test: p = 0.027). However, no changes were observed among the group of cells transfected with MUT-STAT-3'-UTR, suggesting the direct interaction of miR-124 with the 3'UTR region of STAT3 (Fig. 6B). Western blot and qRT-PCR assays showed that

322

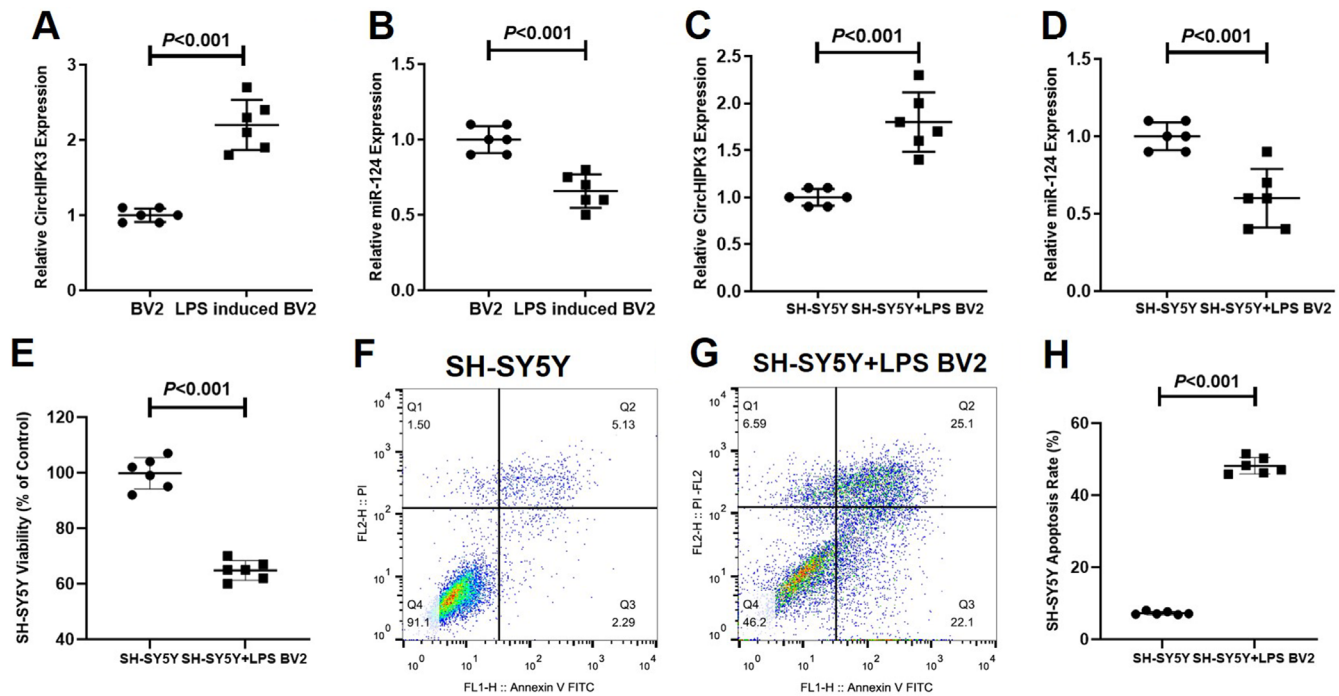Y. Zhang et al. CircHIPK3 in Parkinson's disease

Fig. 2. A. Comparison of relative circular RNA homeodomain interacting protein kinase 3 (circHIPK3) expression between BV2 cells and lipopolysaccharide (LPS)-induced BV2 cells; B. Comparison of relative microRNA-124 (miR-124) expression between BV2 cells and LPS-induced BV2 cells; C. Comparison of relative circHIPK3 expression between SH-SY5Y cells with different treatments; D. Comparison of relative miR-124 expression between SH-SY5Y cells with different treatments; E. Comparison of SH-SY5Y cell viability between SH-SY5Y cells with different treatments; F. Representative figure of the apoptosis rate of SH-SY5Y cells; G. Representative figure of the apoptosis rate of SH-SY5Y cells adding conditioned LP2-BV2 medium; H. Comparison of the apoptosis rates between SH-SY5Y cells with different treatment. Results were statistically analyzed using Mann–Whitney U test. Data were expressed as data point plots, from the minimum to the maximum value (n = 6) for each group. The interval represents the median value. The ends of the interval represent the interquartile range (IQR)

the overexpression of miR-124 inhibited the expression of STAT3 protein and mRNA (Kruskal–Wallis test, H(4) = 19.59, p < 0.001; Dunn's post hoc test: p = 0.030), while miR-124-silenced cells exhibited an elevated STAT3 expression at mRNA and protein levels (Kruskal–Wallis test, H(4) = 19.59, p < 0.001; Dunn's post hoc test: p = 0.024) (Fig. 6C,D).

CircHIPK3 sponged miR-124 in LPS-induced BV2 cells

To elucidate whether circHIPK3 could act as a miR-124 sponge in LPS-induced BV2 cells, a prediction for the potential target miRNA of circHIPK3 was conducted using circBase (Fig. 7A). The relative activity of luciferase in the WT-circHIPK3 reporter-contained BV2 cells was significantly increased and reduced, respectively (Kruskal–Wallis test, H(3) = 19.51, p < 0.001) after miR-124 mimic (Dunn's post hoc test: p = 0.017) and anta-miR-124 transfections (Dunn's post hoc test: p = 0.030, Fig. 7B), suggesting an interaction between circHIPK3 and miR-124. To explore the connection between circHIPK3 and the expression of miR-124, we overexpressed and silenced the expression of circHIPK3 in BV2 cells. Suppressed and elevated miR-124 expression in cells with circHIPK3 overexpression and silencing were observed in our northern blot results. Moreover, the expressions of circHIPK3 in circHIPK3-overexpressed (Kruskal–Wallis

test, H(3) = 19.51, p < 0.001, Dunn's post hoc test: p = 0.025) and circHIPK3-silenced cells (Dunn's post hoc test: p = 0.033) were verified using qRT-PCR (Fig. 7D, Table 2 – No. 27–29).

To further verify the sponge between circHIPK3 and miR-124, a FISH experiment was conducted. As shown in Fig. 8A, the co-localization of circHIPK3 and miR-124 was discovered in BV2 cells. Moreover, in comparison to the IgG-treated control group, the argonaute RISC catalytic component 2 (Ago2) antibody-treated group exhibited dramatically elevated circHIPK3 and miR-124 expression (Fig. 8B, miR-124 RIP: Kruskal–Wallis test, H(2) = 11.67, p < 0.001; circHIPK3: Kruskal–Wallis test, H(2) = 11.63, p < 0.001; miR-124: Dunn's post hoc test, p = 0.008; circHIPK3: Dunn's post hoc test: p = 0.006, respectively). The RNA pull-down results showed that miR-124 and circHIPK3 could pull down each other (miR-124: Mann–Whitney U test, U = 0, p = 0.002; circHIPK3: Mann–Whitney U test, U = 0, p = 0.002, Fig. 8C,D), suggesting a direct sponge between miR-124 and circHIPK3 (Table 2 – No. 30–33).

Discussion

Recently, researchers looking for a consensus opinion in regard to the pathogenesis of PD have been devoting more attention to the role of the inflammatory component.[34]
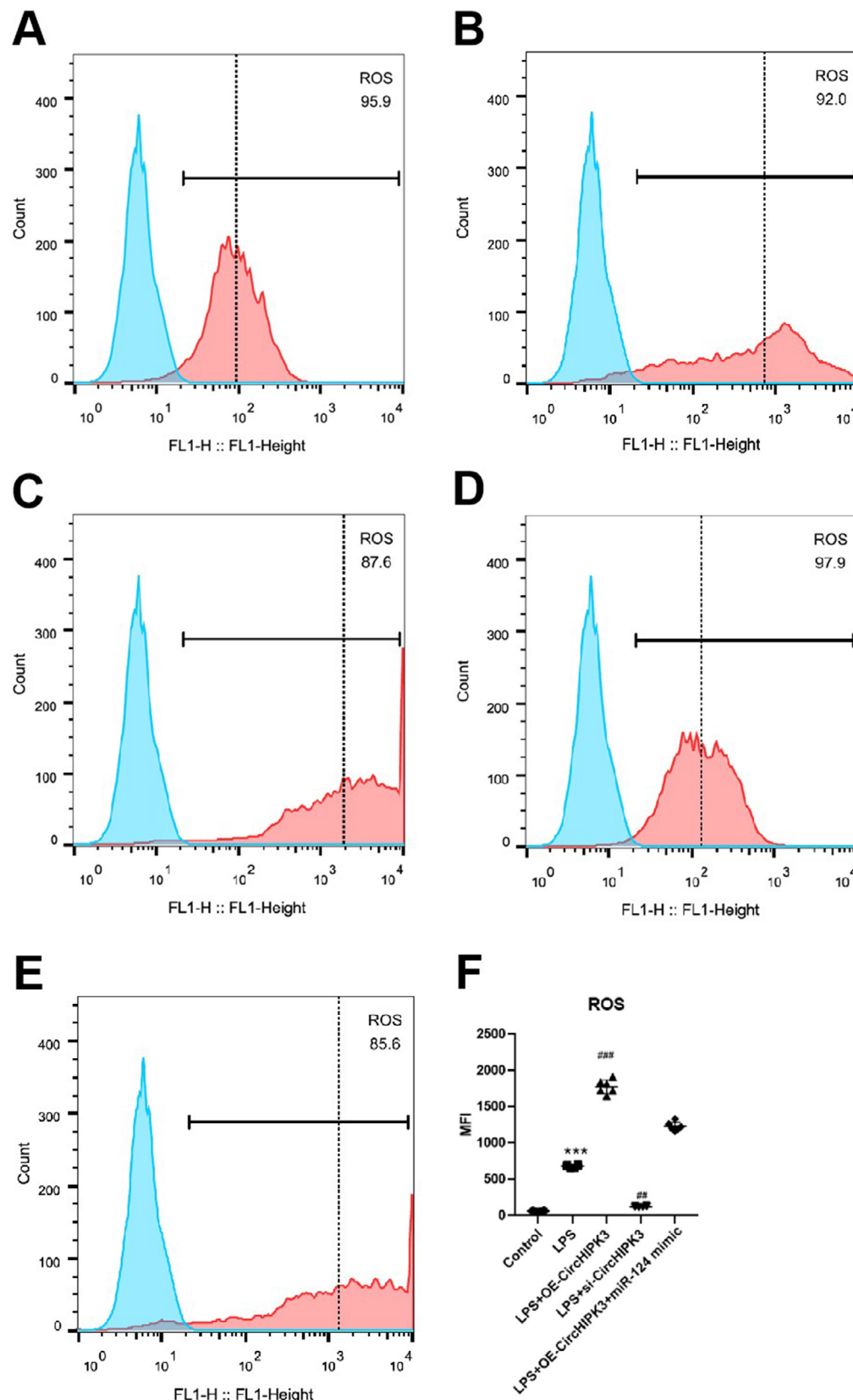
Fig. 3. Reactive oxygen species (ROS) production following circular RNA homeodomain interacting protein kinase 3 (circHIPK3) transfection. A. Production of ROS in the control group; B. Production of ROS in the lipopolysaccharide (LPS) group; C. Production of ROS in the LPS+OE-circHIPK3 group; D. Production of ROS in the LPS+si-circHIPK3 group; E. Production of ROS in the LPS+OE-circHIPK3+microRNA-124 (miR-124) mimic group; F. Quantitative analysis of ROS production in each group (*** $p < 0.001$ compared to the control group; ### $p < 0.001$ and ## $p < 0.01$ compared to the LPS group). Results were statistically analyzed using Kruskal–Wallis test followed by Dunn's post hoc test. Data were expressed as data point plots, from the minimum to the maximum value (n = 6) for each group. The interval represents the median value. The ends of the interval represent the interquartile range (IQR)

MFI – mean fluorescence intensity; OE – overexpression; si – silencing.

Studies have demonstrated that PD is not only a neurodegenerative problem related to the progressive loss of dopamine but also a neuroinflammatory disease.[35] As a kind of programmed cell death, pyroptosis was associated with inflammatory responses dependent on caspase-1 and activated by NLRP3.[36] It has been identified that the activation of pyroptosis was positively correlated with inflammatory cytokine production, which plays an important role in the pathogenesis of PD.[37] However, the process of pyroptosis regulation in PD remains poorly understood.
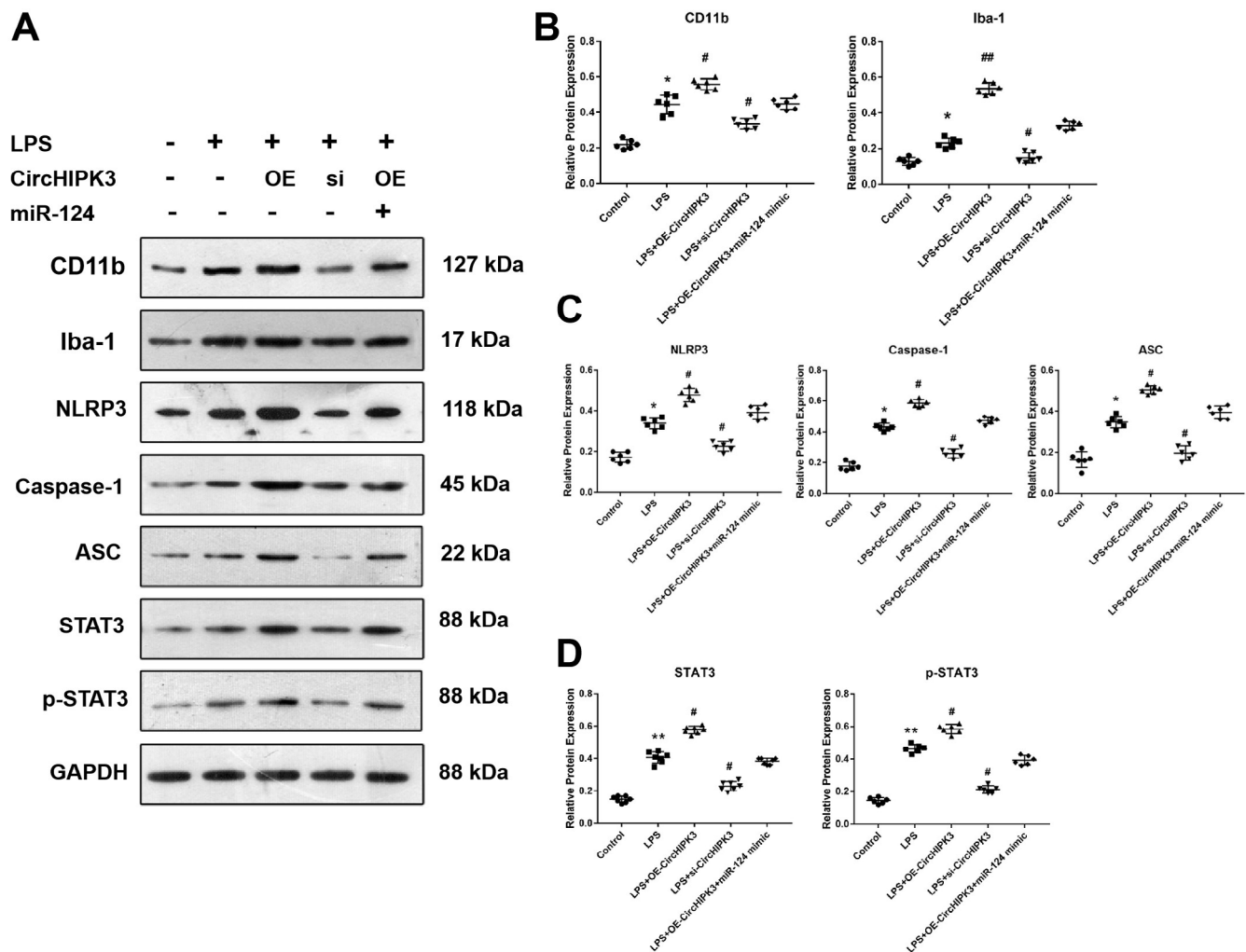
Fig. 4. Circular RNA homeodomain interacting protein kinase 3 (circHIPK3) promoted microglial activation and pyroptosis through the activation of signal transducer and activator of transcription 3 (STAT3) signaling. A. Representative blots showing the production of cluster of differentiation molecule 11b (CD11b) and ionized calcium-binding adapter molecule 1 (Iba-1), pyroptosis-related factors, family pyrin domain containing 3 (NLRP3), caspase-1, apoptosis-associated speck-like protein containing C-terminal caspase recruitment domain (ASC), STAT3, and phosphorylated STAT3 (p-STAT3) in the cells after the indicated treatment; B. Expression of microglia markers CD11b and Iba-1 after the circHIPK3 transfection; C. Expression of pyroptosis-related factors, NLRP3, caspase-1, and ASC after the circHIPK3 transfection; D. Expression of STAT3 and p-STAT3 after the circHIPK3 transfection (* $p < 0.05$ compared to control; # $p < 0.05$ and ## $p < 0.01$ compared to the lipopolysaccharide (LPS) group). Results were statistically analyzed using Kruskal–Wallis test followed by Dunn's post hoc test. Data were expressed as data point plots from the minimum to the maximum value (n = 6) for each group. The interval represents the median value. The ends of the interval represent the interquartile range (IQR)

GAPDH – glyceraldehyde-3-phosphate dehydrogenase; OE – overexpression; si – silencing.

In the present study, we found that a novel circular RNA, circHIPK3, was elevated in PD patients, LPS-induced BV2 cells and conditioned SH-SY5Y medium. Furthermore, our study suggested that circHIPK3 is related to the activation and inflammation of LPS-induced BV2 microglia. Additionally, our study demonstrated that circHIPK3 could directly interact with miR-124 and subsequently regulate the expression of STAT3, which is affected by miR-124, and activate the generation of a NLRP3 inflammasome. An accurately controlled expression of miR-124 was tightly connected with the neurogenesis, physiology and normal development of the CNS. Additionally, miR-124 participated in keeping α-synuclein within a physiologic level. The association of dopaminergic neurodegeneration with significantly reduced expression of miR-124 in the brain

was observed in PD patients and PD-induced animals using 1-Methyl-4-phenyl-1,2,3,6-tetrahydropyridine (MPTP).[38] Furthermore, researchers discovered that miR-124 was significantly involved in the neuroinflammation involved in the pathogenesis of PD.[39] Therefore, the connection between circHIPK3 and miR-124 in PD patients was explored. We observed a significantly decreased expression of miR-124 in PD patients, BV2 cells after LPS stimulation, and SH-SY5Y cells treated with CM collected from LPA-treated BV2 cells. Through bioinformatic analysis, the potential binding sites between miR-124 and circHIPK3 were discovered and verified using a dual-luciferase assay. At the same time, a negative correlation between the expression of circHIPK3 and miR-124 was observed, and the over-expression of miR-124 significantly reversed the expression
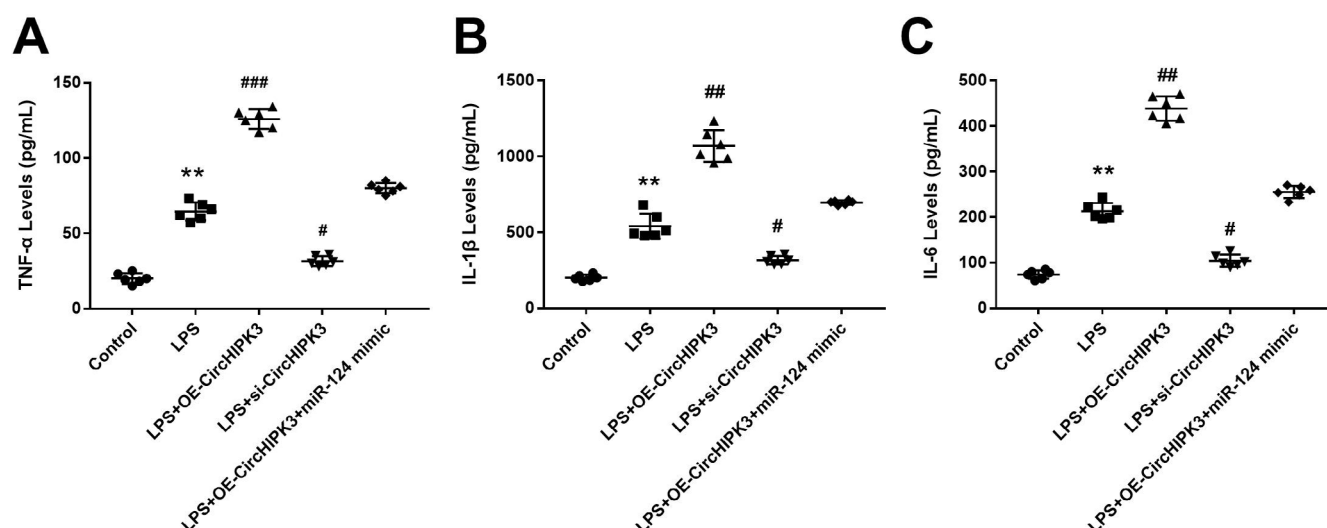
Fig. 5. Effect of circular RNA homeodomain interacting protein kinase 3 (circHIPK3) on the expression of inflammatory factors. A–C. Representative bar graphs showing the expression of tumor necrosis factor alpha (TNF-α) (A), inteleukin (IL)-1β (B) and IL-6 (C) in cells after different treatments (** $p < 0.01$ compared to the control group; # $p < 0.05$, ## $p < 0.01$ and ### $p < 0.001$ compared to the lipopolysaccharide (LPS) group). Results were statistically analyzed using Kruskal–Wallis test followed by Dunn's post hoc test. Data were expressed as data point plots from the minimum to the maximum value (n = 6) for each group. The interval represents the median value. The ends of the interval represent the interquartile range (IQR)
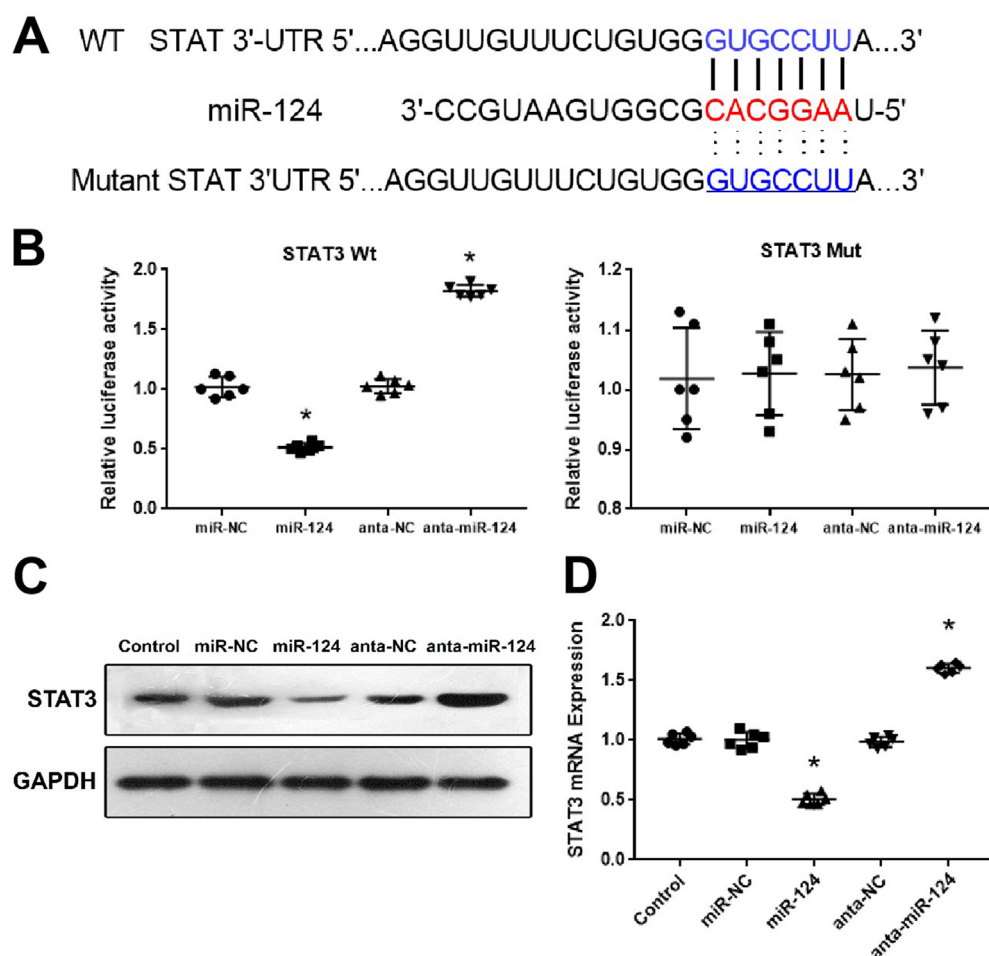
OE – overexpression; si – silencing.

Fig. 6. MicroRNA-124 (miR-124) directly targeted signal transducer and activator of transcription 3 (STAT3). A. Binding sites of miR-124 with the 3'-UTR of STAT3 and the sequences of MUT-STAT3-3'-UTR; B. Relative luciferase activities of cells co-transfected with WT-STAT3-3'UTR or MUT-STAT3-3'-UTR with miR-124 mimic or miR-NC or anta-miR-124 or anta-NC (* $p < 0.05$ compared to miR-NC); C. Representative western blot results showing the expression of STAT3 in cells with different treatments; D. Representative bar graph showing the mRNA levels of STAT3 after different transfections (* $p < 0.05$ compared to controls). Results were statistically analyzed using Kruskal–Wallis test followed by Dunn's post hoc test. Data were expressed as data point plots from the minimum to the maximum value (n = 6) for each group. The interval represents the median value. The ends of the interval represent the interquartile range (IQR)

GAPDH – glyceraldehyde-3-phosphate dehydrogenase; WT – wild-type; MUT – mutant-type; NC – negative control.

of circHIPK3-induced CD11b and Iba-1. On the other hand, the activation of STAT3 was observed in microglia after brain ischemia,[40] as well as in spinal cord microglia after nerve injury.[41] The activation of STAT3 was significantly involved in the inflammatory responses and inflammation induced by thrombin in microglia in vitro.[42] The blockage of STAT3 pathway activation was associated with the suppression of neuroinflammation mediated by microglia.[42]

A

WT CircHIPK3 5'-...AUCAAACUCAGUCAAGUGCCUUU...-3'
|||||||
miR-124   3'-CCGUAAGUGGCGCACGGAAU-5'
::::::::
MUT CircHIPK3 5'-...AUCAAACUCAGUCAAGCAGGCCU...-3'

B

CircHIPK3 Wt — Relative luciferase activity (miR-NC, miR-124, anta-NC, anta-miR-124)

CircHIPK3 Mut — Relative luciferase activity (miR-NC, miR-124, anta-NC, anta-miR-124)

C

pcDNA CircHIPK3 si-NC si-CircHIPK3

miR-124

U6

D

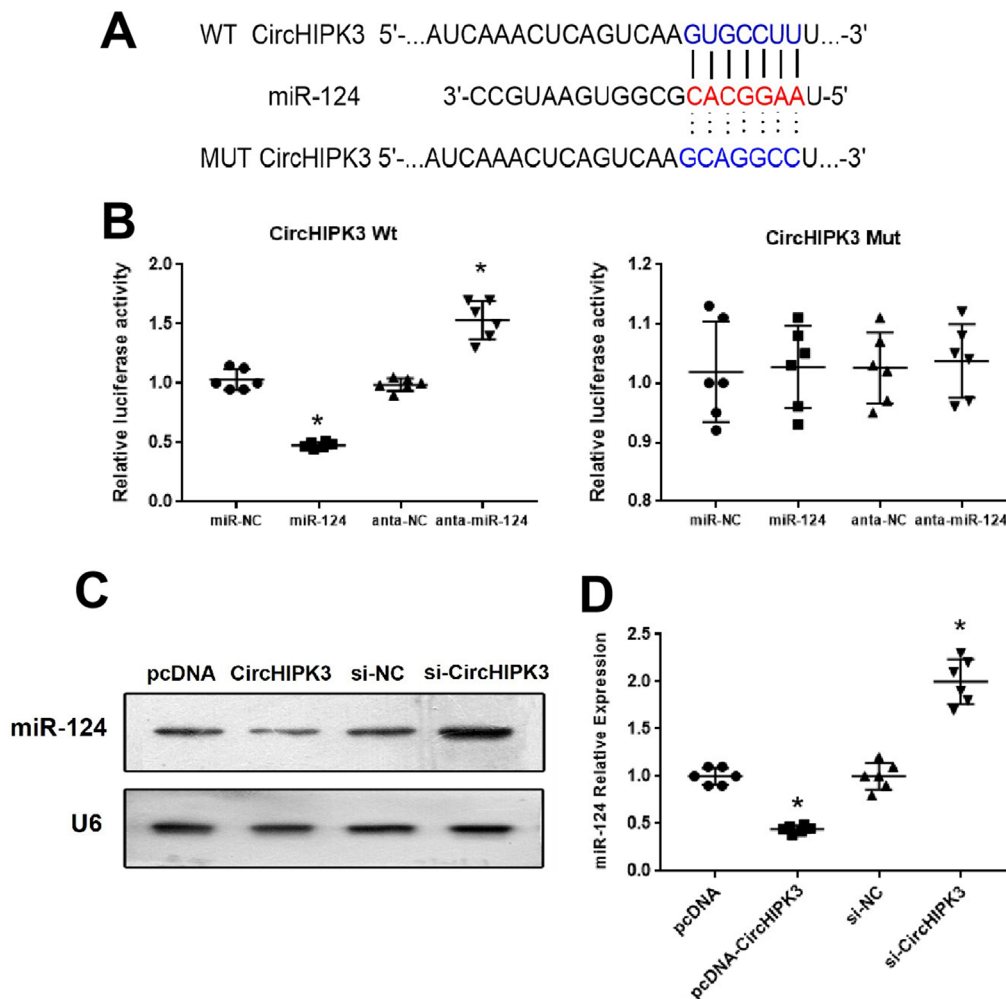miR-124 Relative Expression (pcDNA, pcDNA-CircHIPK3, si-NC, si-CircHIPK3)

Fig. 7. The interaction between circular RNA homeodomain interacting protein kinase 3 (circHIPK3) and microRNA-124 (miR-124). A. Predicted binding site of circHIPK3 and miR-124; B. Representative bar graph showing the relative activities of luciferase in cells after the indicated transfection (* p < 0.05 compared to miR-negative control (miR-NC)); C. Representative northern blot results showing miR-124 expression in cells with the indicated treatment; D. Representative bar graph showing the mRNA levels of circHIPK3 in the cells after the indicated treatment (* p < 0.05 compared to plasmid cloning (pcDNA)). Results were statistically analyzed using Kruskal–Wallis test followed by Dunn's post hoc test. Data were expressed as data point plots from the minimum to the maximum value (n = 6) for each group. The interval represents the median value. The ends of the interval represent the interquartile range (IQR)

si – silencing.

We found that the overexpression of circHIPK3 increased the total STAT3 as well as p-STAT3 expression. In conclusion, our observations suggest that circHIPK3 exerts a promotive effect on the activation of microglia through impairing miR-124/STAT3/NLRP3 expression.

Reactive oxygen species are deeply involved in the development, expression and transduction of signals in cells.[43] However, an excessive production or accumulation of ROS in cells results in damage to cell membranes, DNA and protein molecules.[44] The cell death caused by excessive ROS production is activated by the mitochondrial apoptosis pathway.[45] Due to lower antioxidative enzymes and higher oxidative metabolism, neurons are more sensitive to ROS-induced cell death.[46,47] In recent years, oxidative stress and excessive ROS production were observed in the pathogenesis of PD and found to be significantly associated with the degeneration of dopaminergic neurons.[48] In vitro and in vivo studies have revealed that inflammatory responses and oxidative stress significantly participated in the activation of glial cells, as well as the subsequent damage to dopaminergic neurons.[49] Herein, we observed that the overexpression of circHIPK3 enhanced ROS production in LPS-stimulated BV2 cells, and adding miR-124 alleviated this effect. The circHIPK3 has been demonstrated to increase ROS production in other studies. For example,

the overexpression of circHIPK3 significantly promoted hypoxia/reoxygenation-induced cardiomyocyte cell injury by increasing intracellular ROS production.[50] In addition, silencing circHIPK3 partially impaired inflammation and oxidative injuries caused by LPS.[51]

Limitations

There were several limitations of the present study that should be taken into account. First, we only detected the expression of circHIPK3 in PD patients. The investigation of other circRNAs may reveal much more information about non-coding RNAs in PD progression. Second, we only performed in vitro cell studies; thus, further in vivo animal studies are needed to verify this finding.

Conclusions

We demonstrated that the circHIPK3 expression was increased in PD patients as well as LPS-induced BV2 cells. The circHIPK3 could promote the inflammatory response by sponging miR-124 and affecting the activation of STAT-3- and NLRP3-mediated inflammatory signaling pathways. In addition, circHIPK3 silencing decreased ROS
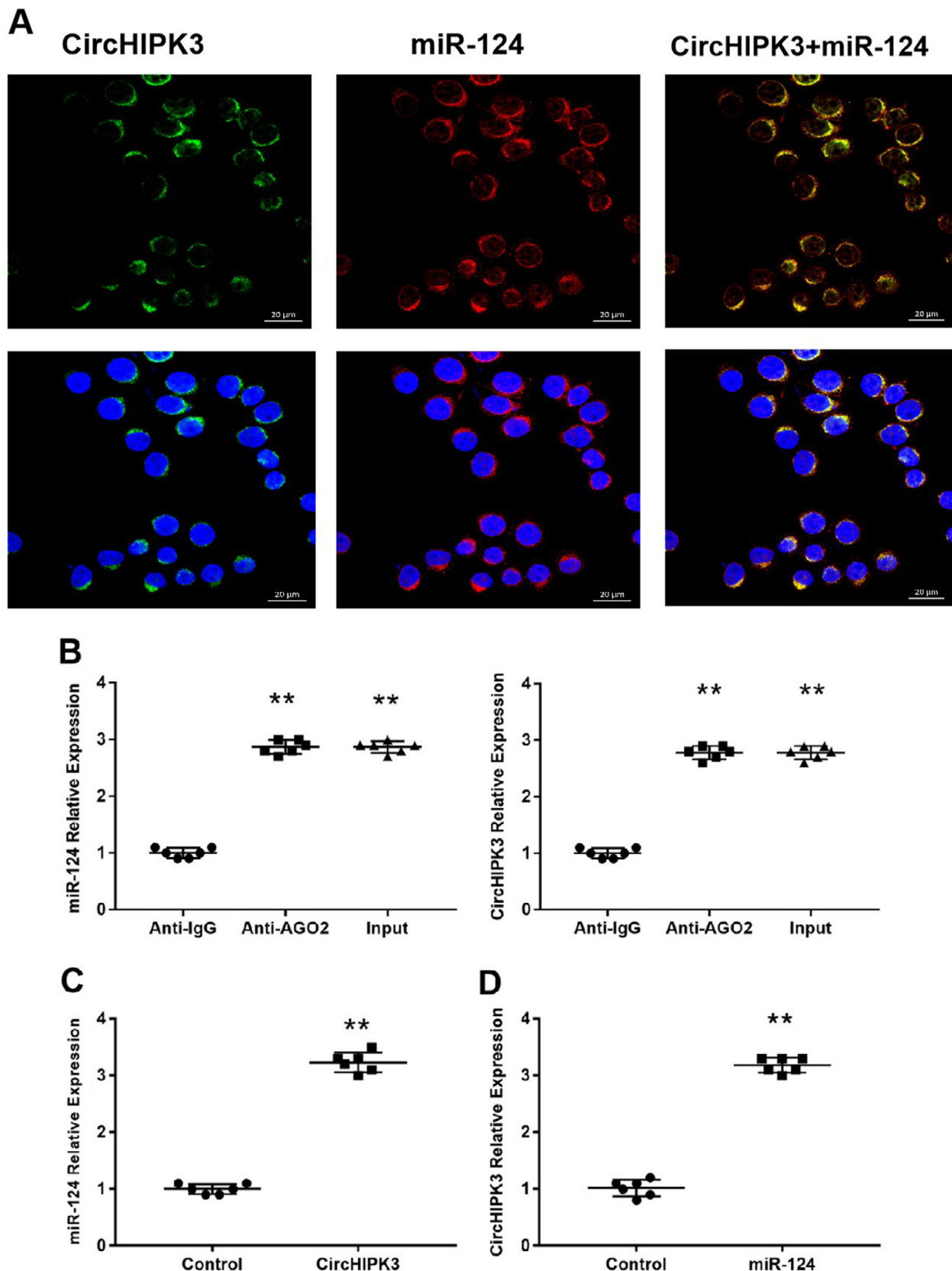
Fig. 8. A. Representative images showing the localization of circular RNA homeodomain interacting protein kinase 3 (circHIPK3) and microRNA-124 (miR-124) in BV2 cells (green: circHIPK3, red: miR-124, blue: 4′,6-diamidino-2-phenylindole (DAPI), scale bar: 20 μm); B. Representative summarized results showing the relative expression of miR-124 and circHIPK3 in cells after different treatments (** $p < 0.01$ compared to anti-immunoglobulin G (anti-IgG)). Results were statistically analyzed using Kruskal–Wallis test followed by Dunn's post hoc test. Data were expressed as data point plots; C,D. Representative bar graphs showing the relative levels of miR-124 (C) and circHIPK3 (D) in pellets pulled down with circHIPK3 (C) and miR-124 (D), and their controls (** $p < 0.01$ compared to controls). Results were statistically analyzed using |Mann–Whitney U test. Data were expressed as data point plots from the minimum to the maximum value ($n = 6$) for each group. The interval represents the median value. The ends of the interval represent the interquartile range (IQR)

production. This study provides evidence that circHIPK3 functions as a miR-124 sponge to STAT3, and could be a potential target in the treatment of PD.

Supplementary materials

The supplementary materials are available at https://doi.org/10.5281/zenodo.7074360. The package contains the following files:

Supplementary File. Results of normality and homogeneity tests for respective Figures.

Supplementary Table. Results of statistical tests.

ORCID iDs

Yu-Juan Zhang https://orcid.org/0000-0003-0358-1691
Wen-Kai Zhu https://orcid.org/0000-0002-5651-7709
Fa-Ying Qi https://orcid.org/0000-0002-4046-6687
Feng-Yuan Che https://orcid.org/0000-0001-6551-2072

References

1. Jankovic J, Tan EK. Parkinson's disease: Etiopathogenesis and treatment. *J Neurol Neurosurg Psychiatry*. 2020;91(8):795–808. doi:10.1136/jnnp-2019-322338
2. Antony PMA, Diederich NJ, Krüger R, Balling R. The hallmarks of Parkinson's disease. *FEBS J*. 2013;280(23):5981–5993. doi:10.1111/febs.12335
3. Kalia LV, Lang AE. Parkinson's disease. *Lancet*. 2015;386(9996):896–912. doi:10.1016/S0140-6736(14)61393-3
4. Gelders G, Baekelandt V, Van der Perren A. Linking neuroinflammation and neurodegeneration in Parkinson's disease. *J Immunol Res*. 2018;2018:4784268. doi:10.1155/2018/4784268
5. Liu B, Gao HM, Hong JS. Parkinson's disease and exposure to infectious agents and pesticides and the occurrence of brain injuries: Role of neuroinflammation. *Environ Health Perspect*. 2003;111(8):1065–1073. doi:10.1289/ehp.6361
6. Yan YQ, Fang Y, Zheng R, Pu JL, Zhang BR. NLRP3 inflammasomes in Parkinson's disease and their regulation by parkin. *Neuroscience*. 2020;446:323–334. doi:10.1016/j.neuroscience.2020.08.004
7. Subhramanyam CS, Wang C, Hu Q, Dheen ST. Microglia-mediated neuroinflammation in neurodegenerative diseases. *Semin Cell Dev Biol*. 2019;94:112–120. doi:10.1016/j.semcdb.2019.05.004
8. Xu L, He D, Bai Y. Microglia-mediated inflammation and neurodegenerative disease. *Mol Neurobiol*. 2016;53(10):6709–6715. doi:10.1007/s12035-015-9593-4
9. Gustin A, Kirchmeyer M, Koncina E, et al. NLRP3 inflammasome is expressed and functional in mouse brain microglia but not in astrocytes. *PLoS One*. 2015;10(6):e0130624. doi:10.1371/journal.pone.0130624
10. Chen LL, Yang L. Regulation of circRNA biogenesis. *RNA Biol*. 2015;12(4):381–388. doi:10.1080/15476286.2015.1020271
11. Du WW, Zhang C, Yang W, Yong T, Awan FM, Yang BB. Identifying and characterizing circRNA-protein interaction. *Theranostics*. 2017;7(17):4183–4191. doi:10.7150/thno.21299
12. Zhang Z, Yang T, Xiao J. Circular RNAs: Promising biomarkers for human diseases. *EBioMedicine*. 2018;34:267–274. doi:10.1016/j.ebiom.2018.07.036
13. Zhang Y, Zhao Y, Liu Y, Wang M, Yu W, Zhang L. Exploring the regulatory roles of circular RNAs in Alzheimer's disease. *Transl Neurodegener*. 2020;9(1):35. doi:10.1186/s40035-020-00216-z
14. Wang Y, Wang Y, Zhang H, He Z. The role of circular RNAs in brain and stroke. *Front Biosci (Landmark Ed)*. 2021;26(5):36. doi:10.52586/4923
15. Kong F, Lv Z, Wang L, et al. RNA-sequencing of peripheral blood circular RNAs in Parkinson disease. *Medicine (Baltimore)*. 2021;100(23):e25888. doi:10.1097/MD.0000000000025888
16. Kuo MC, Liu SCH, Hsu YF, Wu RM. The role of noncoding RNAs in Parkinson's disease: Biomarkers and associations with pathogenic pathways. *J Biomed Sci*. 2021;28(1):78. doi:10.1186/s12929-021-00775-x
17. Hanan M, Simchovitz A, Yayon N, et al. A Parkinson's disease circRNAs resource reveals a link between circSLC8A1 and oxidative stress. *EMBO Mol Med*. 2020;12(9):e11942. doi:10.15252/emmm.201911942

18. Kumar L, Shamsuzzama, Jadiya P, Haque R, Shukla S, Nazir A. Functional characterization of novel circular RNA molecule, circzip-2 and its synthesizing gene zip-2 in *C. elegans* model of Parkinson's disease. *Mol Neurobiol*. 2018;55(8):6914–6926. doi:10.1007/s12035-018-0903-5
19. Ghosal S, Das S, Sen R, Basak P, Chakrabarti J. Circ2Traits: A comprehensive database for circular RNA potentially associated with disease and traits. *Front Genet*. 2013;10(4):283. doi:10.3389/fgene.2013.00283
20. Zheng Q, Bao C, Guo W, et al. Circular RNA profiling reveals an abundant circHIPK3 that regulates cell growth by sponging multiple miRNAs. *Nat Commun*. 2016;7(1):11215. doi:10.1038/ncomms11215
21. Lian C, Sun J, Guan W, et al. Circular RNA circHIPK3 activates macrophage NLRP3 inflammasome and TLR4 pathway in gouty arthritis via sponging miR-561 and miR-192. *Inflammation*. 2021;44(5):2065–2077. doi:10.1007/s10753-021-01483-2
22. Fan S, Hu K, Zhang D, Liu F. Interference of circRNA HIPK3 alleviates cardiac dysfunction in lipopolysaccharide-induced mice models and apoptosis in H9C2 cardiomyocytes. *Ann Transl Med*. 2020;8(18):1147. doi:10.21037/atm-20-5306
23. Wang L, Luo T, Bao Z, Li Y, Bu W. Intrathecal circHIPK3 shRNA alleviates neuropathic pain in diabetic rats. *Biochem Biophys Res Commun*. 2018;505(3):644–650. doi:10.1016/j.bbrc.2018.09.158
24. Angelopoulou E, Paudel YN, Piperi C. miR-124 and Parkinson's disease: A biomarker with therapeutic potential. *Pharmacol Res*. 2019;150:104515. doi:10.1016/j.phrs.2019.104515
25. Wang H, Ye Y, Zhu Z, et al. MiR-124 regulates apoptosis and autophagy process in MPTP model of Parkinson's disease by targeting to Bim. *Brain Pathol*. 2016;26(2):167–176. doi:10.1111/bpa.12267
26. Li N, Pan X, Zhang J, et al. Plasma levels of miR-137 and miR-124 are associated with Parkinson's disease but not with Parkinson's disease with depression. *Neurol Sci*. 2017;38(5):761–767. doi:10.1007/s10072-017-2841-9
27. Zhang F, Yao Y, Miao N, Wang N, Xu X, Yang C. Neuroprotective effects of microRNA 124 in Parkinson's disease mice. *Arch Gerontol Geriatr*. 2022;99:104588. doi:10.1016/j.archger.2021.104588
28. Hillmer EJ, Zhang H, Li HS, Watowich SS. STAT3 signaling in immunity. *Cytokine Growth Factor Rev*. 2016;31:1–15. doi:10.1016/j.cytogfr.2016.05.001
29. Przanowski P, Dabrowski M, Ellert-Miklaszewska A, et al. The signal transducers Stat1 and Stat3 and their novel target Jmjd3 drive the expression of inflammatory genes in microglia. *J Mol Med*. 2014;92(3):239–254. doi:10.1007/s00109-013-1090-5
30. Tanaka S, Ishii A, Ohtaki H, Shioda S, Yoshida T, Numazawa S. Activation of microglia induces symptoms of Parkinson's disease in wild-type, but not in IL-1 knockout mice. *J Neuroinflammation*. 2013;10(1):907. doi:10.1186/1742-2094-10-143
31. Jiang Q, Tang G, Zhong X, Ding D, Wang H, Li J. Role of Stat3 in NLRP3/caspase-1-mediated hippocampal neuronal pyroptosis in epileptic mice. *Synapse*. 2021;75(12):e22221. doi:10.1002/syn.22221
32. Hirsch EC, Hunot S. Neuroinflammation in Parkinson's disease: A target for neuroprotection? *Lancet Neurol*. 2009;8(4):382–397. doi:10.1016/S1474-4422(09)70062-6
33. Kustrimovic N, Marino F, Cosentino M. Peripheral immunity, immunoaging and neuroinflammation in Parkinson's disease. *Curr Med Chem*. 2019;26(20):3719–3753. doi:10.2174/0929867325666181009161048
34. Pajares M, I. Rojo IA, Manda G, Boscá L, Cuadrado A. Inflammation in Parkinson's disease: Mechanisms and therapeutic implications. *Cells*. 2020;9(7):1687. doi:10.3390/cells9071687
35. Lünemann JD, Malhotra S, Shinohara ML, Montalban X, Comabella M. Targeting inflammasomes to treat neurological diseases. *Ann Neurol*. 2021;90(2):177–188. doi:10.1002/ana.26158
36. Hirsch EC, Vyas S, Hunot S. Neuroinflammation in Parkinson's disease. *Parkinsonism Relat Disord*. 2012;18:S210–S212. doi:10.1016/S1353-8020(11)70065-7
37. Tansey MG, Goldberg MS. Neuroinflammation in Parkinson's disease: Its role in neuronal death and implications for therapeutic intervention. *Neurobiol Dis*. 2010;37(3):510–518. doi:10.1016/j.nbd.2009.11.004
38. Kanagaraj N, Beiping H, Dheen ST, Tay SSW. Downregulation of miR-124 in MPTP-treated mouse model of Parkinson's disease and MPP iodide-treated MN9D cells modulates the expression of the calpain/cdk5 pathway proteins. *Neuroscience*. 2014;272:167–179. doi:10.1016/j.neuroscience.2014.04.039

39. Liu F, Qiu F, Chen H. miR-124-3p ameliorates isoflurane-induced learning and memory impairment via targeting STAT3 and inhibiting neuroinflammation. *Neuroimmunomodulation*. 2021;28(4):248–254. doi:10.1159/000515661

40. Planas AM, Soriano MA, Berruezo M, et al. Induction of Stat3, a signal transducer and transcription factor, in reactive microglia following transient focal cerebral ischaemia. *Eur J Neurosci*. 1996;8(12):2612–2618. doi:10.1111/j.1460-9568.1996.tb01556.x

41. Lindborg JA, Tran NM, Chenette DM, et al. Optic nerve regeneration screen identifies multiple genes restricting adult neural repair. *Cell Rep*. 2021;34(9):108777. doi:10.1016/j.celrep.2021.108777

42. Huang C, Ma R, Sun S,et al. JAK2-STAT3 signaling pathway mediates thrombin-induced proinflammatory actions of microglia in vitro. *J Neuroimmunol*. 2008;204(1–2):118–125. doi:10.1016/j.jneuroim.2008.07.004.

43. Kolodkin A, Sharma RP, Colangelo AM, et al. ROS networks: Designs, aging, Parkinson's disease and precision therapies. *NPJ Syst Biol Appl*. 2020;6(1):34. doi:10.1038/s41540-020-00150-w

44. Zorov DB, Juhaszova M, Sollott SJ. Mitochondrial reactive oxygen species (ROS) and ROS-induced ROS release. *Physiol Rev*. 2014;94(3):909–950. doi:10.1152/physrev.00026.2013

45. Sinha K, Das J, Pal PB, Sil PC. Oxidative stress: The mitochondria-dependent and mitochondria-independent pathways of apoptosis. *Arch Toxicol*. 2013;87(7):1157–1180. doi:10.1007/s00204-013-1034-4

46. Vicente-Gutiérrez C, Jiménez-Blasco D, Quintana-Cabrera R. Intertwined ROS and metabolic signaling at the neuron-astrocyte interface. *Neurochem Res*. 2021;46(1):23–33. doi:10.1007/s11064-020-02965-9

47. Kennedy KAM, Sandiford SDE, Skerjanc IS, Li SSC. Reactive oxygen species and the neuronal fate. *Cell Mol Life Sci*. 2012;69(2):215–221. doi:10.1007/s00018-011-0807-2

48. Guo J, Zhao X, Li Y, Li G, Liu X. Damage to dopaminergic neurons by oxidative stress in Parkinson's disease (review). *Int J Mol Med*. 2018;41(4):1817–1825. doi:10.3892/ijmm.2018.3406

49. Miller RL, James-Kracke M, Sun GY, Sun AY. Oxidative and inflammatory pathways in Parkinson's disease. *Neurochem Res*. 2009;34(1):55–65. doi:10.1007/s11064-008-9656-2

50. Qiu Z, Wang Y, Liu W, et al. CircHIPK3 regulates the autophagy and apoptosis of hypoxia/reoxygenation-stimulated cardiomyocytes via the miR-20b-5p/ATG7 axis. *Cell Death Discov*. 2021;7(1):64. doi:10.1038/s41420-021-00448-6

51. Fan S, Hu K, Zhang D, Liu F. Interference of circRNA HIPK3 alleviates cardiac dysfunction in lipopolysaccharide-induced mice models and apoptosis in H9C2 cardiomyocytes. *Ann Transl Med*. 2020;8(18):1147–1147. doi:10.21037/atm-20-5306